

RESEARCH PAPER

Excess manganese differentially inhibits photosystem I versus II in *Arabidopsis thaliana*

R. Millaleo¹, M. Reyes-Díaz^{2,3}, M. Alberdi^{2,3,*}, A. G. Ivanov⁴, M. Krol⁴ and N. P. A. Hüner⁴

¹ Programa de Doctorado en Ciencias de Recursos Naturales, Universidad de La Frontera, Temuco, Chile

² Departamento de Ciencias Químicas y Recursos Naturales; Facultad de Ingeniería, Ciencias y Administración, Universidad de La Frontera, Temuco, Chile

³ Center of Plant, Soil Interaction and Natural Resources Biotechnology, Scientific and Technological Bioresource Nucleus (BIOREN-UFRO), Universidad de La Frontera, Temuco, Chile

⁴ Department of Biology and The Biotron Centre for Experimental Climate Change Research, Western University, London, Ontario, N6A 5B7, Canada

* To whom correspondence should be addressed. E-mail: malberdi@ufro.cl

Received 2 August 2012; Revised 18 October 2012; Accepted 30 October 2012

Abstract

The effects of exposure to increasing manganese concentrations (50–1500 μM) from the start of the experiment on the functional performance of photosystem II (PSII) and photosystem I (PSI) and photosynthetic apparatus composition of *Arabidopsis thaliana* were compared. In agreement with earlier studies, excess Mn caused minimal changes in the PSII photochemical efficiency measured as F_v/F_m , although the characteristic peak temperature of the $S_{2/3}Q_B^-$ charge recombinations was shifted to lower temperatures at the highest Mn concentration. SDS-PAGE and immunoblot analyses also did not exhibit any significant change in the relative abundance of PSII-associated polypeptides: PSII reaction centre protein D1, Lhcb1 (major light-harvesting protein of LHCII complex), and PsbO (OEC33, a 33 kDa protein of the oxygen-evolving complex). In addition, the abundance of Rubisco also did not change with Mn treatments. However, plants grown under excess Mn exhibited increased susceptibility to PSII photoinhibition. In contrast, *in vivo* measurements of the redox transients of PSI reaction centre (P700) showed a considerable gradual decrease in the extent of P700 photooxidation (P700⁺) under increased Mn concentrations compared to control. This was accompanied by a slower rate of P700⁺ re-reduction indicating a downregulation of the PSI-dependent cyclic electron flow. The abundance of PSI reaction centre polypeptides (PsaA and PsaB) in plants under the highest Mn concentration was also significantly lower compared to the control. The results demonstrate for the first time that PSI is the major target of Mn toxicity within the photosynthetic apparatus of *Arabidopsis* plants. The possible involvement mechanisms of Mn toxicity targeting specifically PSI are discussed.

Key words: Chlorophyll fluorescence, Mn toxicity, photosystem I, PSI-associated proteins, PSII-associated proteins, redox state of P700.

Introduction

Manganese (Mn) is one of the most abundant metals in the Earth's crust and although it is an important essential micro-nutrient for all photosynthetic organisms can be also toxic when it is present in excess (Mukhopadhyay and Sharma,

1991; Marschner, 1995). Mn is considered the second most phytotoxic element, after aluminium (Al), affecting negatively the physiological and biochemical properties of plant species (Foy *et al.*, 1978, Foy, 1984; Millaleo *et al.*, 2010). An

excess of this metal occurs in acid soils with low pH (<5.5) and/or under reducing conditions (Marschner, 1995; Schaaf *et al.*, 2002), where Mn^{2+} is the predominant solution species and available ion to plant cells (Bradl, 2004). Thus, a Mn excess results in a sharp decrease in shoot height, biomass accumulation, and total leaf area of a woody species (*Populus cathayana*, Lei *et al.*, 2007), a reduction of the dry weights (DW) of both shoots and roots in ryegrass cultivars (*Lolium perenne*, Mora *et al.*, 2009), and *Trifolium repens* (Rosas *et al.*, 2007). Furthermore, excess Mn can result in oxidative stress as indicated by the accumulation of H_2O_2 (Demirevska-Kepova *et al.*, 2004; Lei *et al.*, 2007), high levels of apoplastic H_2O_2 -consuming peroxidases (Fecht-Christoffers *et al.*, 2003), and high level of lipid peroxidation (Mora *et al.*, 2009). Mn stress induced an enhancement of antioxidant enzyme activity in leaves of legumes (González *et al.*, 1998), and it was also demonstrated in perennial ryegrass (Mora *et al.*, 2009) and woody species (Lei *et al.*, 2007). More recently, a proteomic and transcriptomic studies have demonstrated that chloroplastic proteins important for CO_2 fixation and photosynthesis were of lower abundance upon Mn stress of cowpea (Führs *et al.*, 2008).

Mn has an important role in both the structure and functions of the photosynthetic apparatus (Mukhopadhyay and Sharma, 1991). Mn is a constitutive element associated with the oxygen-evolving complex of photosystem II (PSII), an important multiprotein pigment complex embedded in the thylakoid membranes (Hankamer *et al.*, 1997; Enami *et al.*, 2008). Therefore, the Mn cluster, together with other ions and extrinsic proteins that constitute the oxygen-evolving complex, is required to oxidize water and reduce P680, the reaction centre of PSII (Kern and Renger, 2007; Ferreira *et al.*, 2004; Rutherford and Boussac, 2004). In conjunction with photosystem I (PSI) and linear electron transport, these reducing equivalents (electrons) are used primarily in the conversion of CO_2 into carbohydrate (Ferreira *et al.*, 2004). In addition, Mn is indispensable as a cofactor for various enzymes involved in redox reactions such as Mn-superoxide dismutase, an essential enzyme involved in protection against oxidative stress in plants (Burnell, 1988; Bowler *et al.*, 1994).

A number of studies have suggested that chloroplasts and photosynthesis are the major targets of Mn toxicity. Indeed, increased amounts of Mn have been reported for chloroplasts isolated from Mn-stressed common bean (González and Lynch, 1999) and rice leaves (Lidon *et al.*, 2004). Distinctive ultrastructural changes showing swelling of granal and stromal thylakoids have been also observed in the chloroplasts of *Citrus volkameriana* (Papadakis *et al.*, 2007) and maize plants (Doncheva *et al.*, 2009) under Mn excess. It has been demonstrated that high Mn accumulation is associated with inhibition of the net photosynthesis and carboxylation efficiency in various plant species. The decline of photosynthesis is considered as one of the major mechanisms constituting the toxic effects of excess Mn and is proposed as an early indicator for Mn toxicity in tobacco (Nable *et al.*, 1988), rice (Lidon *et al.*, 2004) and wheat (Macfie and Taylor, 1992). Reduced CO_2 assimilation induced by excess Mn was also reported for common bean (González and Lynch, 1997), deciduous broad

leaved trees (Kitao *et al.*, 1997a), and seedlings of *Citrus grandis* (Li *et al.*, 2010). Interestingly, the maximum photochemical efficiency of PSII (F_v/F_m) was not substantially affected by Mn accumulation in various plant species over a wide range of leaf Mn concentrations (Nable *et al.*, 1988; Kitao *et al.*, 1997b; Subrahmanyam and Rathore, 2000; Hajiboland and Hasani, 2007; Doncheva *et al.*, 2009).

The reduction in photosynthesis by excess leaf Mn has been generally attributed to modification of ribulose-1,5-bisphosphate carboxylase/oxygenase (Rubisco; Ohki, 1984; Houtz *et al.*, 1988; McDaniel and Toman, 1994; Kitao *et al.*, 1997b). It has been demonstrated that a high level of Mn affects primarily the activity rather than the amount of Rubisco (Houtz *et al.*, 1988; Chatterjee *et al.*, 1994) and the presence of excess Mn induces enhanced oxygenase activity (Jordan and Ogren, 1983). In addition, the decline of photosynthesis under Mn stress conditions was also ascribed to peroxidative impairment of photosynthetic enzyme activities caused by polyphenol oxidation products (Vaughn and Duke, 1984; Panda *et al.*, 1987).

In spite of these studies, the mechanisms of Mn toxicity causing a decrease in CO_2 assimilation are still not well understood. In addition, very limited information concerning the toxic effect(s) of excess Mn on the polypeptide composition of both PSII and, especially, PSI is available. Therefore, the objective of this study was to evaluate the role of specific Mn-induced changes in the structure and function of PSII and PSI, which could help to understand the mechanisms by which Mn excess may cause a decrease of CO_2 assimilation in *Arabidopsis thaliana*.

Materials and methods

Plant material and growth conditions

Seeds of *A. thaliana* (wild type Columbia) were germinated in a substrate mix (82.5% sphagnum peat moss, 12.5% perlite, 5% vermiculite-Pro-Mix, Premier Tech Horticulture) in controlled environment growth cabinets (model GCW15, Environmental Growth Chambers, Chagrin Falls, OH, USA) with a photosynthetical active radiation (PAR) of 250 $\mu\text{mol photons m}^{-2} \text{s}^{-1}$, 20/20 °C day/night temperatures, 50% relative humidity, and 8/16 light/dark cycle to prevent flowering. Water was supplied every 5 days. After 15 days, seedlings were transplanted separately in pots with vermiculite and placed in trays. Each tray containing seven pots (one plant per pot) were supplied with Hoagland nutrient solution for 2 weeks before applying the Mn treatments.

Manganese treatments

Manganese treatments included the final concentrations: 18 (control), 50, 500, 1000, and 1500 μM Mn according to Delhaize *et al.* (2007). Manganese was applied as $MnCl_2 \cdot 4H_2O$. Control plants exposed to 18 μM Mn as the optimal dose for Mn for *Arabidopsis* (Cailliatte *et al.*, 2010). The five Mn treatments were grown in five labelled trays, with 500 ml of Hoagland's solution. The trays were maintained in controlled environment growth chambers under the same conditions described above. The pH was adjusted to 5.3 with diluted HCl daily and nutrient solution was changed every 5 days. Plants were subjected to these treatments for 21 days before harvest.

Plant growth measurements

Prior to beginning the Mn treatments, three plant samples were dried in a forced-air oven (70 °C, 48 h) and weighed to determine dry weight

(W1) at day 0. Similarly, at the end of the experiment, plants were harvested and collected for dry weight measurements (W2). These data were used to determine mean relative growth rate (RGR) according to [Fernando et al. \(2009\)](#):

$$RGR = \frac{(\ln W2 - \ln W1)}{t2 - t1}$$

as g DW d⁻¹.

Manganese concentration

For Mn chemical analysis, samples of shoot and roots were dry ashed in a muffle furnace at 500 °C for 8 h and digested with 2 M HCl. Manganese was extracted as described by [Sadzawka et al. \(2004\)](#), and the Mn concentration was determined using a simultaneous multi-element atomic absorption spectrophotometer (model 969, Unicam, Cambridge, UK).

Thylakoid preparation, SDS-PAGE, and immunoblotting

Thylakoid membranes for SDS-PAGE were isolated as described earlier ([Krol et al., 1999](#)). Leaf material was ground in cold isolation buffer (50 mM Tricine, 0.4 M sorbitol, 10 mM NaCl, 5 mM MgCl₂, pH 7.8) in a mortar on ice, filtered through two layers of miracloth (typical pore size 22–25 µm; Calbiochem), and centrifuged for 15 min (10,000 g). The supernatant was removed and the pellet was resuspended in cold isolation buffer. Total chlorophyll concentration was measured in 90% (v/v) acetone ([Arnon, 1949](#)). For immunodetection of Rubisco, total leaf proteins were extracted as described in [Rosso et al. \(2009\)](#). Protein content was measured using a BCA protein assay kit (Pierce) by following the absorbance at 562 nm using a spectrophotometer (DU-640, Beckman Coulter). Proteins were separated by SDS-PAGE according to [Laemmli \(1970\)](#), using 15% (w/v) polyacrylamide gel in the presence of 6 M urea in the separating gel. Chloroplast thylakoids were solubilized with SDS (SDS:chlorophyll 20:1) and 15 µg chlorophyll was loaded per lane. All samples for separation of total proteins were loaded on an equal protein basis of 20 µg protein per lane ([Rosso et al. 2009](#)). Immunoblotting was performed by electrophoretically transferring the proteins from SDS-PAGE gel to nitrocellulose membrane (Bio-Rad) according to the method of [Towbin et al. \(1979\)](#). Proteins were probed with antibodies (AgriSera AB, Vanas, Sweden) raised against the reaction centre polypeptides of PSI: PsaA, PsaB (1:2000), the major light-harvesting protein of PSII complex (LHCII) Lhcb1 protein (1:5000), the PSII oxygen-evolving complex extrinsic protein PsbO (33 kDa, 1:2000), the PSII reaction centre protein: D1 and Rubisco (1:5000). As secondary antibodies, goat anti-rabbit IgG conjugated with horseradish peroxidase (Sigma-Aldrich) were used. Polypeptides were detected using enhanced chemiluminescence detection kit (Amersham Biosciences) and visualized by exposing the membrane to X-ray film. Densitometric scanning and analysis of X-ray films from each replicate immunoblot was performed with a Hewlett Packard ScanJet 4200C desktop scanner and ImageJ 1.41o densitometry software (Wayne Rosband, National Institute of Health, USA, <http://rsbweb.nih.gov/ij>).

Measurement of the redox state of P₇₀₀

The redox state of P₇₀₀ was determined *in vivo*, in dark-adapted (20 min) *Arabidopsis* leaves under growth temperature and ambient O₂ and CO₂ conditions using a PAM-101 modulated fluorometer equipped with a dual-wavelength emitter-detector ED-P700DW unit and PAM-102 units ([Klughammer and Schreiber, 1991](#)) as described in detail by [Ivanov et al. \(1998\)](#). Far-red light (λ_{max}=715 nm, 10 W m⁻², Schott filter RG 715) was provided by an FL-101 light source. The redox state of P700 was evaluated as the absorbance change around 820 nm (ΔA_{820–860}) in a custom-designed cuvette. Multiple turnover (MT, 50 ms) and single turnover (ST, half peak 14 µs) saturating flashes were applied with XMT-103 and XST-103 (Walz) power/control units, respectively. The relative functional pool size of intersystem electrons on a P₇₀₀ reaction

centre basis was calculated as the complementary area between the oxidation curve of P700 after either ST or MT pulse excitation (ST and MT areas) and the stationary level of P700 under far-red excitation ([Asada et al., 1993](#); [Ivanov et al., 1998](#)). Capacity of PSI cyclic electron (e⁻) flow was determined as the half time for the dark decay of the P700 signal ([Ivanov et al., 1998](#)).

Modulated chlorophyll fluorescence measurements

Modulated imaging fluorometer (IMAGING-PAM, Heinz Walz, Efeltrich, Germany) was used for capturing the chlorophyll fluorescence images and estimation of the maximal photochemical efficiency of PSII [F_v/F_m = (F_m - F_o)/F_m], effective photochemical efficiency of PSII (Φ_{PSII}), photochemical (qP), and non-photochemical (NPQ) fluorescence quenching parameters using the nomenclature of [van Kooten and Snel \(1990\)](#) as described earlier ([Ivanov et al., 2006a](#)). Control and Mn-treated *Arabidopsis* plants were dark adapted (20 min) and all chlorophyll fluorescence measurements were performed *in vivo* at room temperature. Fluorescence images were captured by a CCD camera (IMAG-K, Allied Vision Technologies) featuring a 640 × 480 pixel CCD chip size and CCTV camera lens (Cosmicar/Pentax F1.2, f = 12 mm). Light emitting diode ring array (IMAG-L) consisting of 96 blue LEDs (470 nm) provided standard modulated excitation intensity of 0.5 µmol quanta m⁻² s⁻¹ (modulation frequency 1–8 Hz) for measuring the basal (F_o) chlorophyll fluorescence and a saturation pulse of 2400 µmol quanta m⁻² s⁻¹ PAR for measuring the maximal chlorophyll fluorescence (F_m). The maximal photochemical efficiency of PSII (F_v/F_m) was determined as (F_m - F_o)/F_m. The effective photochemical efficiency of PSII (Φ_{PSII}) was calculated from the expression (F'_m - F_s)/F'_m ([Genty et al., 1989](#)), photochemical quenching (qP) was calculated as (F'_m - F_s)/(F'_m - F'_o) ([Schreiber et al., 1994](#)), electron transport rate (ETR) was calculated as PAR × 0.5Φ_{PSII} × 0.84 ([Genty et al., 1989](#)), and regulated non-photochemical quenching (Φ_{NPQ}) and constitutive photochemical quenching (Φ_{NO}) was determined according to [Kramer et al. \(2004\)](#). All measurements were performed at 0, 5, 10, 15, and 21 days in plants subjected to the different Mn treatments.

At the end of experiments (21 days), leaves of *Arabidopsis* plants growing under the different Mn treatments and 250 µmol m⁻² s⁻¹ PAR (normal light) were cut and exposed to high light (1000 µmol s⁻¹ m⁻², PAR) at 1, 2, and 4 hours. During each time of exposition, F_v/F_m was determined.

Thermoluminescence measurements

Thermoluminescence (TL) measurements of control and Mn-treated *Arabidopsis* leaves were performed on a personal-computer-based TL data acquisition and analysis system as described earlier ([Ivanov et al., 2001, 2006b](#)). A photomultiplier tube (Hamamatsu R943-02, Hamamatsu Photonics, Shizuoka-ken, Japan) equipped with a photomultiplier power supply (model PS-302, EG&G Electro Optics), and a preamplifier (model C1556-03) was used as a radiation measuring set. The heating rate was 0.6 °C s⁻¹. For identifying the S_{2/3}Q_B⁻ charge recombination peaks, dark-adapted leaf discs were subjected to two consecutive saturating microsecond flashes of white light (1.5 µs peak width at 50% of maximum) applied by a xenon-discharge flash lamp (XST103, Heinz Walz). Dark-adapted leaves (20 minutes at 20 °C) were cooled to 2 °C prior to exposing to the flashes. The nomenclature of [Sane et al. \(2012\)](#) was used for characterization of the TL glow peaks.

Experimental design and statistical analysis

The experimental design is a randomized split design, with 1 species × 5 Mn treatments × 7 replicates for the physiological determinations and 1 species × 5 Mn treatments × 3 replicates × 4 times (0, 1, 2, and 4 hours) for the photoinhibition measurements. Data correspond to the means of replicates for each determination as indicated above. Data were tested in their normality and equal variance by the Shapiro–Wilk test and then data were analysed by a one-way ANOVA. Significant differences between means were established by using the multiple comparisons test

of Tukey's ($P < 0.05$). All analyses were performed with Sigma Stat 2.0 software (SPSS), where differences between the values were considered significant at $P \leq 0.05$.

Results

A statistically significant decrease in total biomass of leaves treated with 500 and 1500 μM Mn concentrations was found compared to the control plants (18 μM Mn), although a decrease of the total leaf biomass was found at all Mn concentrations used. In contrast, root biomass exhibited significant decrease in all treatments ($P < 0.05$, Fig. 1). It should be noted, however, that while the decrease of leaf biomass was only 25% lower at the highest Mn concentration used (1500 μM), the biomass of roots was more affected and demonstrated a 2.5-fold decrease even at the lowest Mn concentration tested (50 μM). This is consistent with the RGR data, where a considerably higher reduction of root RGR was observed compared to leaves across the Mn treatments relative to control plants ($P < 0.05$, Table 1). In addition, visual symptoms of Mn toxicity (chlorosis) in leaves were observed predominantly in the highest Mn treatment (data not shown).

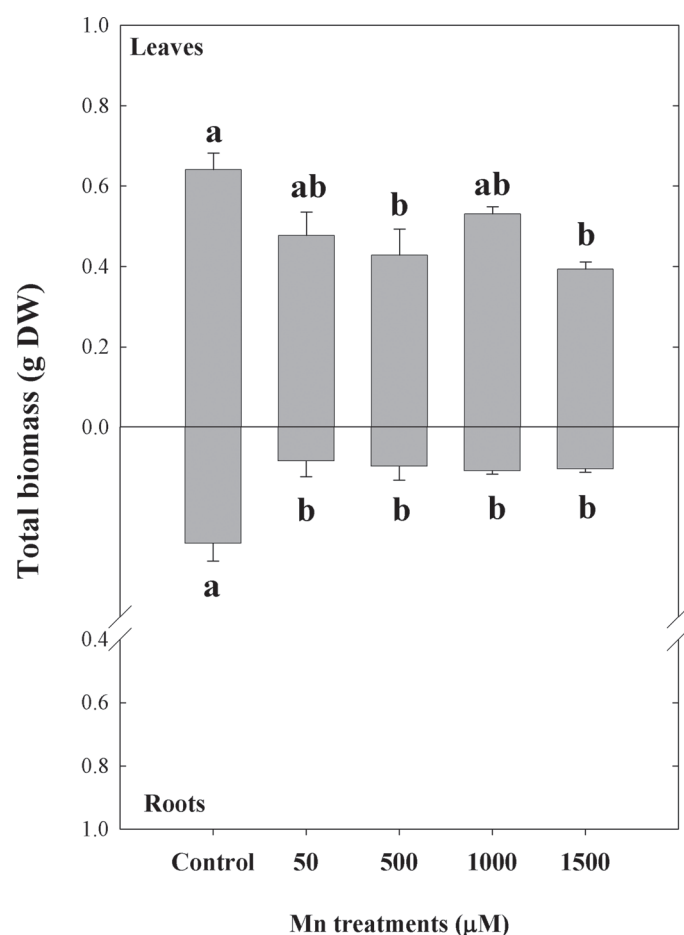


Fig. 1. Total biomass (leaves and roots) of *Arabidopsis thaliana* plants subjected to Mn treatments at the end of experiment (21 days). Different lower-case letters indicate significant differences between the Mn treatments ($P \leq 0.05$).

Table 1. Relative growth rates of *Arabidopsis thaliana* (leaves and roots) growing at increased Mn treatments. Plants were grown under acidic conditions (pH 5.3) for 21 d. Different lower-case letters indicate statistically significant differences between the Mn treatments ($P < 0.05$).

Mn treatment (μM)	Relative growth rate (g DW d ⁻¹)	
	Leaves	Roots
Control	0.069 ± 0.001 ^a	0.206 ± 0.006 ^a
50	0.068 ± 0.003 ^a	0.071 ± 0.005 ^b
500	0.046 ± 0.006 ^b	0.053 ± 0.006 ^b
1000	0.059 ± 0.003 ^{a,b}	0.064 ± 0.007 ^b
1500	0.040 ± 0.004 ^b	0.057 ± 0.004 ^b

Analysis of the total Mn amount in plants exposed to increasing Mn concentrations have demonstrated a gradual increase of Mn in leaves and roots (Fig. 2). However, while Mn concentrations of roots reached values up to ~8100 mg kg⁻¹ Mn at the highest Mn treatment, which represents a 40-fold increase of Mn, the increased accumulation of Mn in leaves was much lower (15-fold) compared to roots (Fig. 2). Thus, the differential effects of Mn treatments on the total

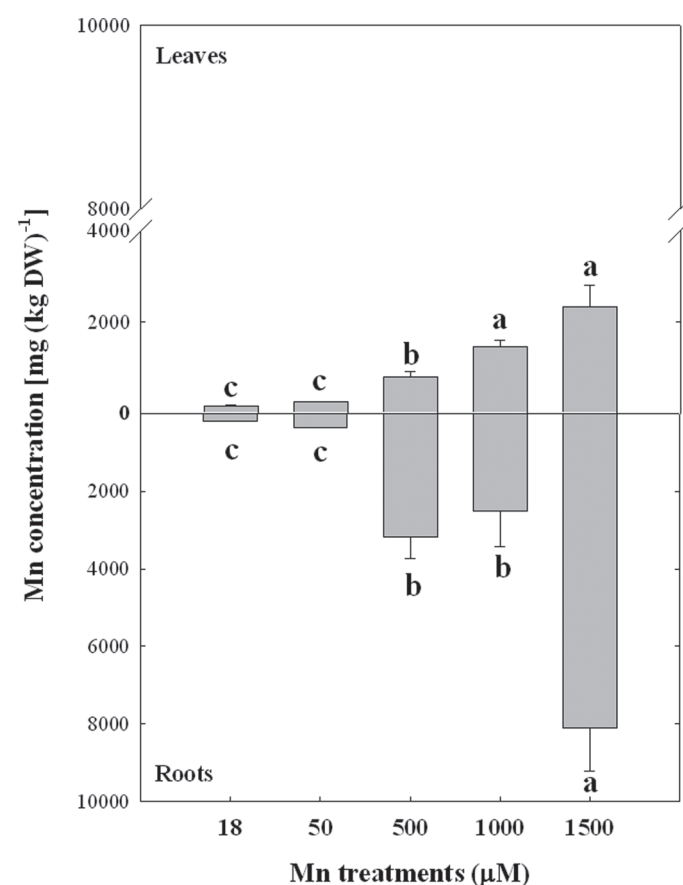


Fig. 2. Mn concentration in leaves and roots of *Arabidopsis thaliana* plants subjected to Mn treatments at the end of experiment (21 days). Different lower-case letters indicate statistically significant differences between the Mn treatments ($P \leq 0.05$).

Table 2. Maximum photochemical efficiency of PSII (F_v/F_m) in leaves of *Arabidopsis thaliana* measured at 0, 5, 10, 15 and 21 days subjected to increasing Mn treatments. Results are means \pm SE of five replicates of two plants each. Different lower-case letters indicate significant differences between the Mn treatments at the same time, while different upper-case letters indicate significant differences between the times at a same Mn treatment ($P < 0.05$).

Mn treatment (μM)	F_v/F_m				
	0 days	5 days	10 days	15 days	21 days
Control	0.803 ^{abA}	0.803 ^{abA}	0.803 ^{abA}	0.803 ^{abA}	0.803 ^{abA}
50	0.806 ^{abA}	0.799 ^{abA}	0.800 ^{abA}	0.800 ^{abA}	0.800 ^{abA}
500	0.803 ^{abA}	0.801 ^{abA}	0.804 ^{abA}	0.787 ^{baA}	0.791 ^{abA}
1000	0.797 ^{abA}	0.805 ^{abA}	0.800 ^{abA}	0.778 ^{bbB}	0.773 ^{bbB}
1500	0.802 ^{abA}	0.798 ^{abA}	0.775 ^{bbB}	0.769 ^{bbBC}	0.756 ^{ccC}

biomass and RGR in leaves and roots could be explained by the higher accumulation of Mn in roots.

The effects of exposure to increasing Mn concentrations on the maximum photochemical efficiency of PSII measured as F_v/F_m in *Arabidopsis* leaves are presented in Table 2. A time-course measurement did not reveal any statistically significant changes of F_v/F_m values at the lower Mn doses (50 and 500 μM) for the entire period of treatment compared to control plants (18 μM Mn). At higher Mn concentrations (1000 and 1500 μM), a small reduction (6%) of F_v/F_m was observed only at a later stage (days 15 and 21) of treatment, the statistically significant ($P < 0.05$) differences being registered at the harvest time (21 days, Table 2). Moreover, minimal Mn-induced changes were detected in the light response curves of photochemical quenching (qP), effective photochemical efficiency of PSII (Φ_{PSII}), and PSII electron transport rates (ETR) even after 21 days of Mn treatments with the highest dose tested (1500 μM , data not shown).

In addition, TL measurements were used as an alternative approach for assessing the effects of Mn excess on the photosynthetic PSII-associated electron transfer reactions especially at its reducing side (Vass and Govindjee, 1996; Sane et al., 2012). Since most of the photosynthetic TL components have been assigned to arise from the reversal of light-driven charge separation in PSII, TL properties of photosynthetic apparatus provide information on the activation energies associated with the back reactions of electron acceptors (Q_A and Q_B) with the electron donors (S_2 and S_3) of PSII (Vass and Govindjee, 1996; Sane, 2004; Sane et al., 2012). The temperature maxima (T_M) of the TL peaks related to the recombination of these charge pairs reflect the activation energies and hence a measure of the redox potentials of the participating oxidized and reduced donors (de Vault and Govindjee, 1990). Typical TL glow curves representing $S_{2/3}Q_B^-$ charge recombinations of control and Mn-treated *Arabidopsis* plants obtained following excitation with two consecutive saturating flashes are shown in Fig. 3. The experimental data summarized in Table 3 indicate that treatment with a Mn dose of 500 μM did not exhibit significant differences of the TL

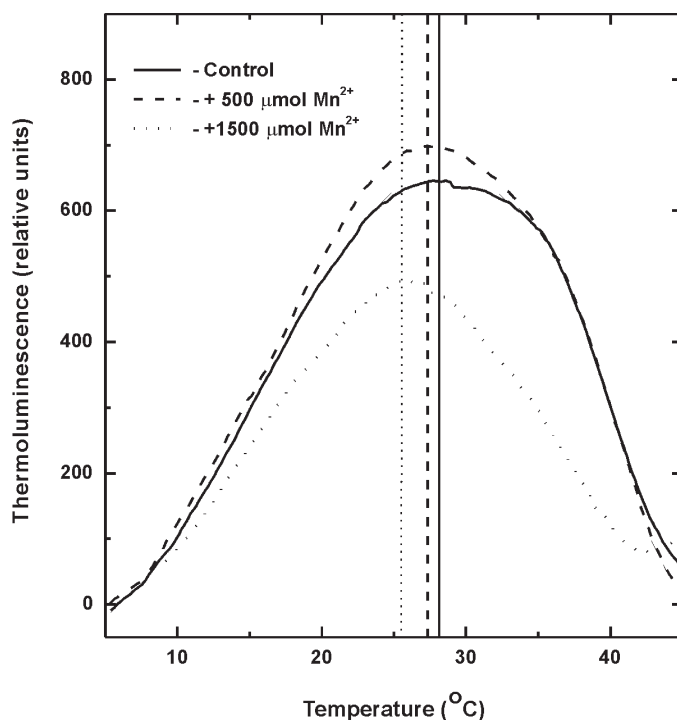


Fig. 3. Thermoluminescence (TL) glow curves of $S_{2/3}Q_B^-$ charge recombinations in control (solid lines) and Mn-treated (dashed lines, 500 μM Mn^{2+} ; dotted lines, 1500 μM Mn^{2+}) *Arabidopsis* leaves after illumination with two single turnover flashes. TL glow curves were recorded immediately after illumination. The presented glow curves are averages from four independent measurements.

peak position, while treatment with the highest concentration (1500 μM) induced a low temperature shift of the T_M to 25.8 $^{\circ}\text{C}$ compared to control plants. Besides this, the amplitudes and the integrated areas of the TL peaks representing the $S_{2/3}Q_B^-$ charge recombination used for assessing the PSII photochemistry was not affected at 500 μM Mn excess, but the overall TL yield was significantly reduced (45%) in plants treated with 1500 μM Mn compared to controls (Table 3).

To further test whether this small but significant Mn-induced effect on PSII photochemistry had physiological implications under additional stress conditions, *Arabidopsis*

Table 3. Characteristic thermoluminescence peak emission temperatures (T_M) and the overall TL emission area (A) of $S_{2/3}Q_B^-$ glow peaks of control and Mn-treated (21 days) *Arabidopsis* plants. The samples (leaf disks) were dark adapted for 30 min then cooled to 2 $^{\circ}\text{C}$ and subsequently illuminated with two single turnover flashes of white light. The peak areas are presented as a percentage of the total thermoluminescence light emission in control leaves. Values are mean \pm SE calculated from four independent experiments.

Mn treatment (μM)	T_M ($^{\circ}\text{C}$)	A (%)
Control	28.7 \pm 1.1	100.0
500	29.1 \pm 1.3	106.2 \pm 7.6
1500	25.8 \pm 0.9	54.5 \pm 7.9

Table 4. Effect of high light treatments (photon flux density 1000 $\mu\text{mol photons m}^{-2} \text{s}^{-1}$ for 1, 2, and 4 hours) on the maximal photochemical efficiency of PSII measured as F_v/F_m in control *Arabidopsis thaliana* leaves and plants exposed for 21 days to different Mn doses. Results are mean \pm SE of five repetitions in three leaves of two plants each. Time 0 was measured in plants subjected to 250 $\mu\text{mol m}^{-2} \text{s}^{-1}$ photon flux density. Different upper-case letters indicate significant differences between the times of exposure at the same Mn treatment ($P < 0.05$).

Irradiance exposition time (h)	F_v/F_m		
	Control	500 $\mu\text{M Mn}$	1500 $\mu\text{M Mn}$
0	0.815 \pm 0.003 ^A	0.812 \pm 0.004 ^A	0.780 \pm 0.014 ^A
1	0.761 \pm 0.012 ^A	0.750 \pm 0.002 ^A	0.677 \pm 0.014 ^B
2	0.752 \pm 0.007 ^A	0.731 \pm 0.002 ^A	0.619 \pm 0.028 ^B
4	0.685 \pm 0.036 ^A	0.689 \pm 0.004 ^A	0.388 \pm 0.042 ^C

leaves subjected to different Mn treatments for 21 days were exposed to high light stress (Table 4). Indeed, the photoinhibitory effect on PSII, measured as a decrease in F_v/F_m , was much stronger (49%) at the highest Mn treatment (1500 μM) compared to control plants, and 500 μM Mn treated plants exhibited only a 15% decrease in F_v/F_m values after 4 h of exposure to high light (Table 4).

The extent of far-red light-induced absorbance decrease at 820 nm ($\Delta A_{820-860}$) of *Arabidopsis* leaves (Klughammer and Schreiber, 1991; Ivanov et al., 1998, 2006a) was used to estimate the potential functional differences of PSI and photosynthetic electron transport pathways between plants exposed to different Mn treatments. Typical traces representing *in vivo* measurements of oxidation–reduction transients of P_{700} in control and Mn-treated plants are shown in Fig. 4. The relative amount of P_{700}^+ , measured as $\Delta A_{820-860}$, gradually decreased with increasing Mn concentrations and was 30% lower in Mn-treated plants at the highest concentration used (1500 μM , Fig. 4 and Table 5). Concomitantly, kinetic measurements of dark re-reduction of P_{700}^+ after turning off the far-red light, which is thought to reflect the extent and/or capacity for cyclic electron flow around PSI (Maxwell and Biggins, 1976; Ravenel et al., 1994), indicated significantly slower (46%) re-reduction of P_{700}^+ in Mn (1500 μM)-treated plants compared to control plants (Table 5). In addition, the apparent electron donor pool size to PSI (e^-/P_{700}) estimated by measuring single- and multiple-turnover flash-induced $\Delta A_{820-860}$ under steady-state oxidation of PSI by far-red light (Asada et al., 1993; Ivanov et al., 1998) demonstrated a significant decrease in Mn-treated plants (Table 5). This indicates that the pool size of electrons that can be donated to photooxidized P_{700} (P_{700}^+) from the stroma in control plants was 37% higher compared to plants treated with the highest Mn dose (13 electrons per P_{700} , Table 4).

The major photosynthetic components within the thylakoid membranes of control and Mn-treated *Arabidopsis* plants were compared by SDS-PAGE and immunodetection to quantify their relative abundance. Immunoblot analyses did not exhibit any significant Mn-stress-induced changes

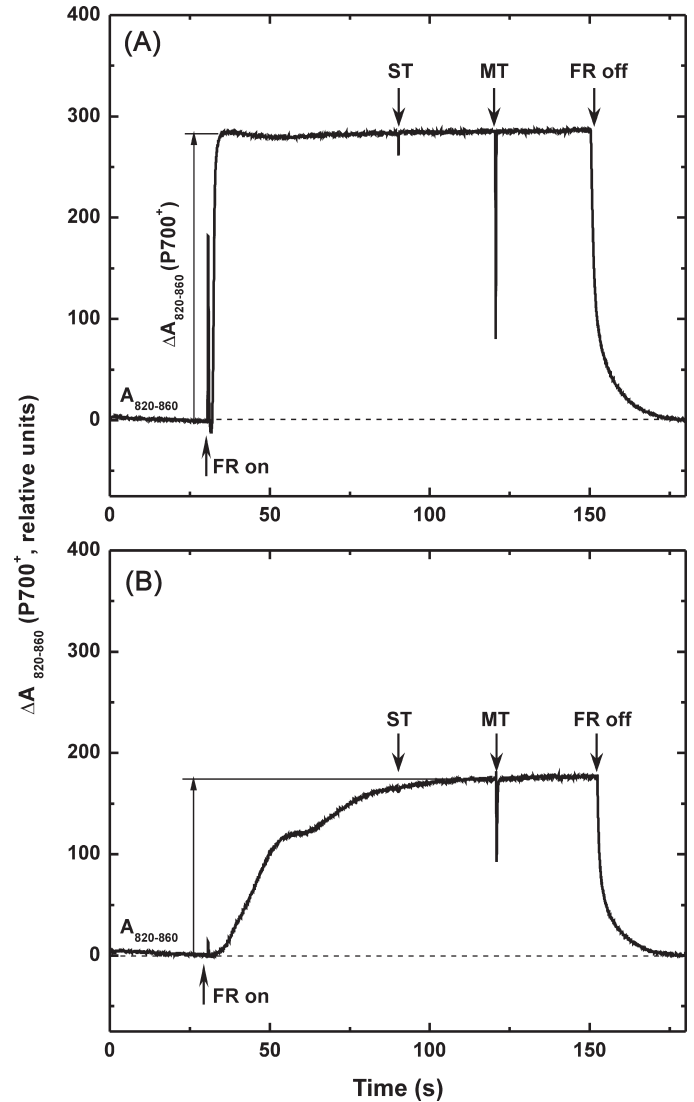


Fig. 4. Typical traces of *in vivo* measurements of P_{700} oxidation by far-red light (FR) in control (A, 18 $\mu\text{M Mn}$) and Mn-treated (B, 1500 $\mu\text{M Mn}$) *Arabidopsis* plants. After reaching a steady state level of P_{700}^+ by FR light, single turnover (ST) and multiple turnover (MT) pulses of white light were applied. Arrows indicate application of ST, MT, and FR light sources. The measurements were performed at the growth temperature of 20 $^{\circ}\text{C}$.

in the relative abundance of PSII-associated polypeptides, as revealed by the densitometry analysis of the immunoblot bands for D1 (the PSII reaction centre protein), Lhcb1 (major light-harvesting protein of LHCII), and PsbO (extrinsic protein of the oxygen-evolving complex (Fig. 5). The abundance of Rubisco was only marginally affected by the Mn treatments. In contrast, the abundance of reaction centre polypeptides of PSI (PsaA and PsaB) was significantly reduced in Mn-treated compared with control thylakoids (Fig. 5A). The densitometric analysis demonstrated that the relative abundance of PsaA and PsaB in Mn-treated *Arabidopsis* was only about 20 and 60%, respectively, of that observed in the control plants (Fig. 5B). Thus, the quantitative analysis of photosynthetic polypeptides clearly indicates that excess Mn has

Table 5. Effects of Mn treatments on far-red light-induced steady state oxidation of P700 ($\Delta A_{820-860}$, P700⁺), the relative intersystem electron donor pool size to PSI ($e^-/P700$) and half times for P700⁺ reduction ($t_{1/2}$) of *Arabidopsis* leaves at 21 days of treatment. Different lower-case letters indicate significant differences between the Mn treatments ($P < 0.05$). MT, multiple turnover; ST, single turnover.

Mn treatment (μM)	$\Delta A_{820-860}$ (P700 ⁺)	$e^-/P700$ (MT _{area} /ST _{area})	$t_{1/2}$ (s)
Control	423.2 ± 7.9 ^a	20.7 ± 0.9 ^a	0.670 ± 0.05 ^b
50	416.4 ± 8.3 ^a	15.7 ± 0.6 ^b	0.812 ± 0.06 ^{a,b}
500	368.4 ± 8.3 ^b	16.4 ± 0.6 ^b	0.938 ± 0.08 ^{a,b}
1000	293.4 ± 8.4 ^c	15.6 ± 0.5 ^b	0.908 ± 0.07 ^{a,b}
1500	292.9 ± 4.2 ^c	13.0 ± 0.3 ^c	0.984 ± 0.08 ^a

a greater effect on PSI-associated proteins rather than PSII. Consequently, the differences in the extent of P700 oxidation (P700⁺) and the kinetics of P700⁺ reduction between control and Mn-treated plants are consistent with the lower levels of PSI-associated immunodetectable PsaA and PsaB protein complexes.

Discussion

In agreement with a number of previous studies examining the effects of Mn stress on various plant species (Alam *et al.*, 2006; Lei *et al.*, 2007; Doncheva *et al.*, 2009; Mora *et al.*, 2009; Stoyanova *et al.*, 2009; Khabaz-Saberi *et al.*, 2010) *Arabidopsis* plants subjected to increasing Mn concentrations, also exhibited a reduction in dry weight of both shoots and roots at doses between 500 and 1500 μM Mn (Fig. 1). The decline in biomass corresponded with a gradual increase of Mn concentrations in both shoot and roots of *Arabidopsis* subjected to excess Mn supply (Fig. 2). It should be noted that the decline of biomass was more pronounced in roots, where even at the lowest Mn treatment (50 μM) the dry weight was 2.5-fold lower compared to leaves. Similar results have been reported by Delhaize *et al.* (2007), where transporter proteins were implicated in the endogenous Mn tolerance of wild-type *Arabidopsis*. More recently, Mora *et al.* (2009) demonstrated that Mn-tolerant ryegrass cultivars accumulated higher Mn concentrations in roots than shoots, while Mn-sensitive cultivars exhibited a greater Mn translocation from roots to shoots. These results are also consistent with studies in legumes such as white clover (*T. repens* L., Rosas *et al.*, 2007). However, in two contrasting populations of *P. cathayana*, acclimated to wet and dry climate exposure to excess Mn caused an increase in Mn content of plant tissues especially in leaves and a visual symptoms of Mn toxicity (chlorosis) at high Mn concentrations (Lei *et al.*, 2007). The chlorosis observed in the present experiments (data not shown) also correspond to a decreased amounts of both Chl a and Chl b could be due to a higher Mn accumulation in leaves after exposure to Mn excess, thus suggesting a damage to the photosynthetic apparatus as reported by Demirevska-Kepova *et al.* (2004).

Interestingly, while reduced CO₂ assimilation induced by excess Mn has been reported in many species and is considered one of the major physiological effects of Mn toxicity (Nable *et al.*, 1988; Macfie and Taylor, 1992; González and Lynch, 1997; Kitao *et al.*, 1997a; Lidon *et al.*, 2004; Li *et al.*, 2010), the functional integrity of the photosynthetic apparatus assessed by the maximum photochemical efficiency of PSII (F_v/F_m) did not decline as a result of exposure to excess Mn in various plant species (Nable *et al.*, 1988; Kitao *et al.*, 1997b; Subrahmanyam and Rathore, 2000; Hajiboland and Hasani, 2007; Doncheva *et al.*, 2009). However, some studies have reported a substantial decrease in F_v/F_m as a result of excess Mn treatment in *Citrus* species (Papadakis *et al.*, 2007; Li *et al.*, 2010), rice (Lidon *et al.*, 2004), Mn-sensitive maize (Doncheva *et al.*, 2009), and cucumber (Feng *et al.*, 2009). Furthermore, Kitao *et al.* (1997b) have shown that the potential maximum photochemical efficiency of PSII (F_v/F_m) is not affected by excess Mn in white birch, although the reduction state of PSII primary electron acceptor (Q_A) was increased at high Mn concentrations. These results clearly indicate that the excess Mn-induced decline in CO₂ assimilation may or may not be accompanied by changes in PSII photochemistry and this response is species dependent. The experimental data presented in this study also failed to demonstrate any substantial effects of excess Mn within a wide range of Mn concentrations on the maximum photochemical efficiency of PSII in *Arabidopsis* plants (Table 2). Assessing the relative abundance of PSII-associated proteins also showed no changes in the immunodetectable amounts of PSII reaction centre protein D1, the light-harvesting chlorophyll-protein complex of PSII (Lhcb1), and the manganese-stabilizing 33-kDa protein of the water splitting complex of PSII (PsbO) polypeptides (Fig. 5) in plants exposed to high Mn concentrations compared to control *Arabidopsis*. However, the observed low temperature shift of the $S_{2/3}Q_B^-$ charge recombination and much lower overall TL emission implies lower redox potential of Q_B (Fig. 3 and Table 3) confirms the suggestion of altered reduction state of PSII acceptor side in Mn-stressed plants (Kitao *et al.*, 1997b). Since Q_A is in quasi-equilibrium with Q_B and the PQ pool, the present results imply that lowering the redox potential of Q_B will decrease the probability for forward electron transfer between the two quinone acceptors by shifting the redox equilibrium between $Q_A^-Q_B$ and $Q_AQ_B^-$ towards $Q_A^-Q_B$ (Minagawa *et al.*, 1999; Ivanov *et al.*, 2002, 2003) in plants exposed to high Mn concentrations.

In addition to the lack of significant inhibitory effects of excess Mn on PSII photochemistry discussed above, an earlier study reported that the photochemistry of photosystem I (PSI) and the photosynthetic electron transport were not significantly affected during early development of Mn toxicity in tobacco plants (Nable *et al.*, 1988). However, a decreased Hill activity in isolated chloroplasts was found in mungbean leaves exposed to toxic Mn concentrations (Sinha *et al.*, 2002). More recently, Li *et al.* (2010) have suggested that Mn excess can effectively impair the whole photosynthetic electron transport chain, thus restricting the production of reducing equivalents and limiting the rate of CO₂ assimilation in *Citrus grandis* seedlings. Despite these few studies,

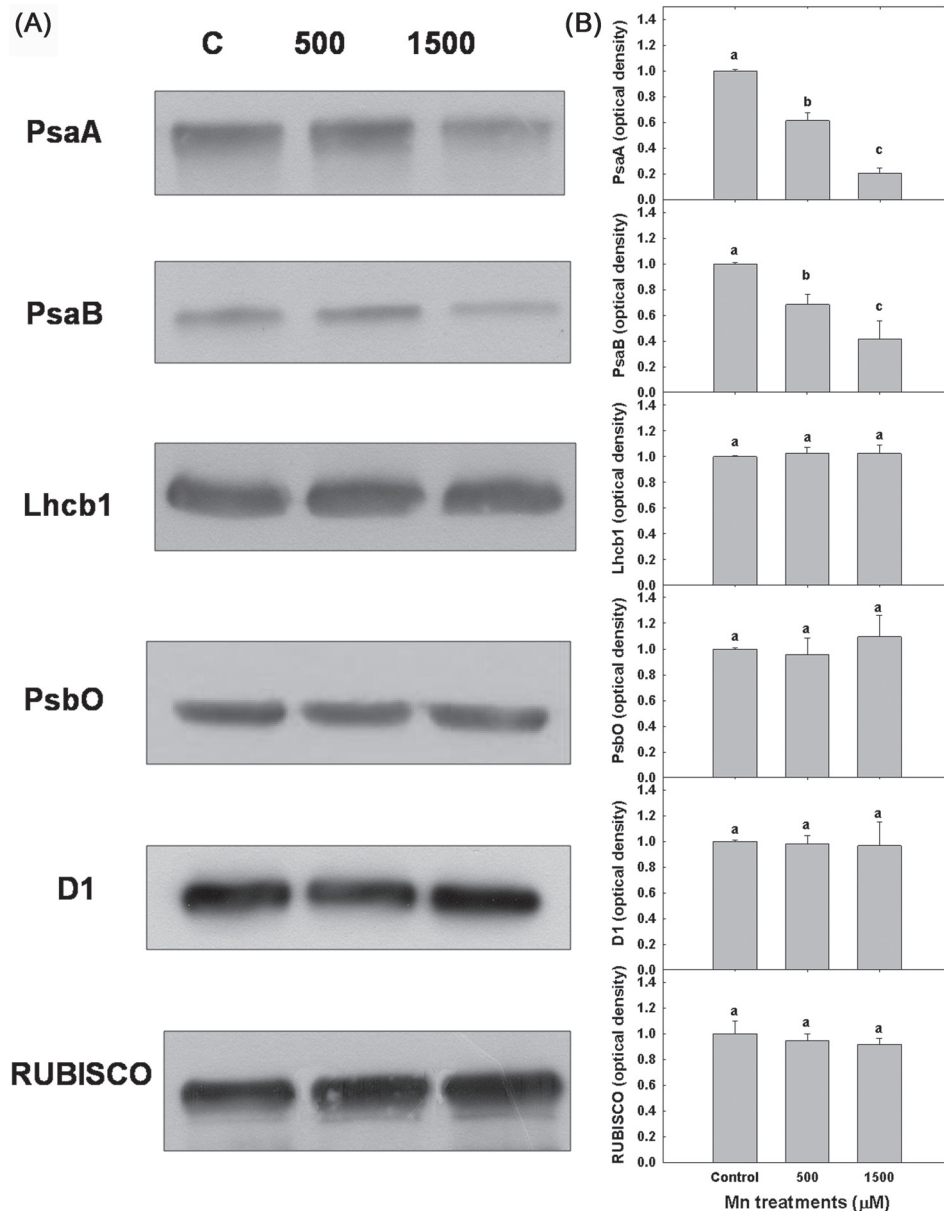


Fig. 5. (A) Representative immunoblots of SDS-PAGE separated proteins from thylakoid membranes probed with antibodies raised against PSI (PsaA and PsaB) and PSII (D1, PsbO, Lhcb1)-associated polypeptides and Rubisco (PbcL) in control (C, 18 μM Mn) and *Arabidopsis* plants treated with 500 and 1500 μM Mn. (B) The relative polypeptide abundance was quantified by densitometric analysis (area × intensity bands) of the immunoblots and the presented data were normalized to the relative abundance of PsaA, PsaB, D1, PsbO, Lhcb1, and PbcL in control *Arabidopsis* plants. Mean ± SE were calculated from three independent experiments. Different lower-case letters indicate significant differences between the Mn treatments ($P < 0.05$).

the potential effect(s) of excess Mn on the functional/structural integrity of PSI remains elusive. As far as is known, the results presented in this study are the first report of an *in vivo* assessment of high Mn concentrations on PSI photochemistry. In contrast to PSII photochemistry, *in vivo* measurements of the oxidation state of P700 (P700⁺) (Klughammer and Schreiber, 1991; Ivanov et al., 1998), the primary donor of PSI demonstrated that the relative amount of oxidizable P700 (P700⁺) decreased by 30% in Mn-treated *Arabidopsis* plants at concentrations above 1000 μM (Fig. 4 and Table 5). The functional impairment of PSI photochemistry by excess Mn was

accompanied by a significant reduction in the abundance of PSI reaction centre polypeptides (PsaA and PsaB, Fig. 5). This clearly indicates that the major target of Mn toxicity within the photosynthetic electron transport chain of *Arabidopsis* is PSI- rather than PSII-related components. The reduced amounts of PSI reaction centre polypeptides PsaA and PsaB would imply acceptor side limitations of the photosynthetic electron transport and this could explain the increased reduction state Q_A in Mn-stressed plants reported earlier (Kitao et al., 1997b). Moreover, the decreased expression of another Fe-containing chloroplastic protein precursor, ferredoxin-1

serving as a terminal electron acceptor of the photosynthetic electron transport, observed in Mn-treated young rice leaves also supports Mn-induced limitations at the acceptor side of PSI (Führes *et al.*, 2010).

One of the major mechanisms considered for Mn toxicity involves the inhibition of other essential cations including Fe, thus suggesting that a Mn-induced Fe deficiency may play a key role in the physiological responses to excess Mn (Foy *et al.*, 1978; Foy, 1984; Kohno *et al.*, 1984). More recently, chloroplast alterations in maize plants exposed to excess Mn (Doncheva *et al.*, 2009) and Mn toxicity in young rice leaves (Führes *et al.*, 2010) have been also ascribed to Mn-induced Fe deficiency rather than to direct Mn-induced oxidative stress. Given that about 80% of the plant Fe is located in the chloroplast (Terry and Abadia, 1986) and that the functional photosynthetic apparatus requires 22–23 iron atoms, of which PSI is the most Fe-abundant component (Ferreira and Straus, 1994), it seems reasonable to assume that the observed lower abundance of PSI reaction centre polypeptides and the associated decline of PSI photochemistry in Mn-treated *Arabidopsis* plants were consequences of a Mn-induced moderate Fe deficiency.

Although light energy is important for photosynthetic processes in plants, an excess of light can be also harmful because it can result in photoinhibition, which can be exacerbated when it is combined with other stresses (Powles, 1984; Aro *et al.*, 1993; Sonoike, 1996). Photoinhibition is a complex phenomenon that may cause damage to the photosynthetic apparatus reducing the photosynthetic efficiency when light conditions exceed the photon requirements for photosynthesis (Murata *et al.*, 2007). It is considered that PSII is the main site of photoinhibition (Aro *et al.*, 1993; Sonoike, 1996; Takahashi and Murata, 2008), being more unstable than PSI, because the D1 protein, one of the two major heterodimeric polypeptides of the PSII reaction centre complex, has a very high light-dependent turnover rate (Aro *et al.*, 1993; Burnap, 2004; Scheller and Haldrup, 2005; Takahashi and Murata, 2008). Earlier reports have shown that the susceptibility to Mn toxicity is strongly dependent on the light intensity and exposure of Mn-treated plants to high light can exacerbate the toxic effect of Mn (Horiguchi, 1988; Nable *et al.*, 1988; González *et al.*, 1998; Clair and Lynch, 2004; Hajiboland and Hasani, 2007). The present results also demonstrate that *Arabidopsis* plants predisposed to high Mn concentrations are more susceptible to photoinhibitory damage of PSII photochemistry in a concentration-dependent manner (Table 4).

Apart from the radiation-less dissipation of excess excitation energy in the chlorophyll pigment bed of LHCII, associated with the formation of the xanthophylls pigment zeaxanthin, which is considered one of the major protective mechanisms against photoinhibitory damage (Horton *et al.*, 1996; Niyogi, 1999), PSI-dependent cyclic electron transport has been also suggested to play a significant role in preventing the photoinhibitory damage of the photosynthetic apparatus during exposure of plants to high light conditions (Munekage *et al.*, 2002; Takahashi *et al.*, 2009). Considering the increased re-reduction rate of P700⁺ in *Arabidopsis* (Table 5), the higher susceptibility of plants exposed to excess

Mn to photoinhibition (Table 4) might be due to lower capacity of PSI-driven cyclic electron flow under conditions of Mn toxicity.

In summary, the results presented in this research demonstrate for the first time that exposure of *Arabidopsis* plants to excess Mn causes specific negative effects on the abundance of polypeptides comprising the reaction centre of PSI, thus resulting in decreased PSI photochemistry and lower capacity for cyclic electron transport, which may be due to a Mn-induced Fe deficiency and may have critical physiological implications under conditions of Mn toxicity in higher plants.

Acknowledgements

This work was supported by the Natural Sciences and Engineering Research Council of Canada (NPAH), a CONICYT internship ‘Pasantías Doctorales en el Extranjero 2010’, the Department of Biology and the Biotron, University of Western Ontario, London, Ontario, Canada, and the Fondecyt project, Government of Chile (no. 1080372).

References

- Alam S, Kodama R, Akiha F, Kamei S, Kawai S. 2006. Alleviation of manganese phytotoxicity in barley with calcium. *Journal of Plant Nutrition* **29**, 59–74.
- Arnon DI. 1949. Copper enzymes in isolated chloroplasts. Polyphenoloxidase in *Beta vulgaris*. *Plant Physiology* **24**, 1–15.
- Aro E-M, Virgin I, Andersson B. 1993. Photoinhibition of photosystem II. Inactivation, protein damage and turnover. *Biochimica et Biophysica Acta* **1143**, 113–134.
- Asada K, Heber U, Schreiber U. 1993. Electron flow to the intersystem chain from stromal components and cyclic electron flow in maize chloroplasts, as determined in intact leaves by monitoring redox change of P700 and chlorophyll fluorescence. *Plant and Cell Physiology* **34**, 39–50.
- Bowler C, VanCamp W, VanMontagu M, Inze D. 1994. Superoxide dismutase in plants. *Critical Reviews in Plant Sciences* **13**, 199–218.
- Bradi H. 2004. Adsorption of heavy metal ions on soils and soils constituents. *Journal of Colloids and Interface Science* **277**, 1–18.
- Burnap RL. 2004. D1 protein processing and Mn cluster assembly in light of the emerging Photosystem II structure. *Physical Chemistry Chemical Physics* **6**, 4803–4809.
- Burnell JN. 1988. The biochemistry of manganese in plants. In: RD Graham, J Hannam, NC Uren, eds, *Manganese in soils and plants*. Dordrecht, The Netherlands: Kluwer Academic Publishers, pp 125–133.
- Cailliatte R, Schikora A, Briat JF, Mari S, Curie C. 2010. High-affinity manganese uptake by the metal transporter NRAMP1 is essential for *Arabidopsis* growth in low manganese conditions. *The Plant Cell* **22**, 904–917.
- Chatterjee C, Nautiyal N, Agarwala SC. 1994. Influence of changes in manganese and magnesium supply on some aspects of wheat physiology. *Soil Science and Plant Nutrition* **40**, 191–197.

- Clair SB St, Lynch JP.** 2004. Photosynthetic and antioxidant enzyme responses of sugar maple and red maple seedlings to excess manganese in contrasting light environments. *Functional Plant Biology* **31**, 1005–1014.
- Delhaize E, Gruber BD, Pittman JK, White RG, Leung H, Miao Y, Jiang L, Ryan PR, Richardson AE.** 2007. A role for the AtMTP11 gene of *Arabidopsis* in manganese transport and tolerance. *The Plant Journal* **51**, 198–210.
- Demirevska-Kepova K, Simova-Stoilova L, Stoyanova Z, Holzer R, Feller U.** 2004. Biochemical changes in barley plants after excessive supply of copper and manganese. *Environmental and Experimental Botany* **52**, 253–266.
- de Vault D, Govindjee.** 1990. Photosynthetic glow peaks and their relationship with the free energy changes. *Photosynthesis Research* **24**, 175–181.
- Doncheva S, Poschenrieder C, Stoyanova Z, Georgieva K, Velichkova M, Barceló J.** 2009. Silicon amelioration of manganese toxicity in Mn-sensitive and Mn-tolerant maize varieties. *Environmental and Experimental Botany* **65**, 189–197.
- Enami I, Okumura A, Nagao R, Suzuki T, Iwai M, Shen JR.** 2008. Structures and functions of the extrinsic proteins of photosystem II from different species. *Photosynthesis Research* **98**, 349–363.
- Fecht-Christoffers MM, Maier P, Horst W.** 2003. Apoplastic peroxidase and ascorbate are involved in manganese toxicity and tolerance of *Vigna unguiculata*. *Physiologia Plantarum* **117**, 237–244.
- Feng J-P, Shi Q-H, Wang X-F.** 2009. Effects of exogenous silicon on photosynthetic capacity and antioxidant enzyme activities in chloroplast of cucumber seedlings under excess manganese. *Agricultural Science in China* **8**, 40–50.
- Fernando DR, Baker AJM, Woodrow IE.** 2009. Physiological responses in *Macadamia integrifolia* on exposure to manganese treatment. *Australian Journal of Botany* **57**, 406–413.
- Ferreira F, Straus NA.** 1994. Iron deprivation in cyanobacteria. *Journal of Applied Phycology* **6**, 199–210.
- Ferreira KN, Iverson TM, Maghlaoui K, Barber J, Iwata S.** 2004. Architecture of the photosynthetic oxygen-evolving center. *Science* **303**, 1831–1838.
- Foy CD.** 1984. Physiological effects of hydrogen, aluminum, and manganese toxicities in acid soils. In: F Adams, editor, *Soil acidity and liming*, 2nd ed. Madison: American Society of Agronomy. pp 57–97.
- Foy CD, Chaney RL, White MC.** 1978. The physiology of metal toxicity in plants. *Annual Review of Plant Physiology* **29**, 511–566.
- Führs H, Behrens C, Gallien S, Heintz D, Van Dorsselaer A, Braun HP, Horst WJ.** 2010. Physiological and proteomic characterization of manganese sensitivity and tolerance in rice (*Oryza sativa*) in comparison with barley (*Hordeum vulgare*). *Annals of Botany* **105**, 1129–1140.
- Führs H, Hartwig M, Molina LEB, Heintz D, Van Dorsselaer A, Braun HP, Horst WJ.** 2008. Early manganese-toxicity response in *Vigna unguiculata* L. – a proteomic and transcriptomic study. *Proteomics* **8**, 149–159.
- Genty B, Briantais J-M, Baker NR.** 1989. The relationship between quantum yield of photosynthetic electron transport and quenching of chlorophyll fluorescence. *Biochimica et Biophysica Acta* **990**, 87–92.
- González A, Lynch JP.** 1997. Effects of manganese toxicity on leaf CO₂ assimilation of contrasting common bean genotypes. *Physiologia Plantarum* **101**, 872–880.
- González A, Lynch JP.** 1999. Subcellular and tissue Mn compartmentation in bean leaves under Mn toxicity stress. *Australian Journal of Plant Physiology* **26**, 811–822.
- González A, Steffen KL, Lynch JP.** 1998. Light and excess manganese. Implication for oxidative stress in common bean. *Plant Physiology* **18**, 493–504.
- Hajiboland R, Hasani BD.** 2007. Effect of Cu and Mn toxicity on chlorophyll fluorescence and gas exchange in rice and sunflower under different light intensities. *Journal of Stress Physiology and Biochemistry* **3**, 4–17.
- Hankamer B, Barber J, Boekema EJ.** 1997. Structure and membrane organization of photosystem II in green plants. *Annual Review of Plant Physiology and Plant Molecular Biology* **48**, 641–671.
- Horiguchi T.** 1988. Mechanism of manganese toxicity and tolerance of plants. VII. Effect of light intensity on manganese-induced chlorosis. *Journal of Plant Nutrition* **11**, 235–245.
- Horton P, Ruban AV, Walters RG.** 1996. Regulation of light harvesting in green plants. *Annual Review of Plant Physiology and Plant Molecular Biology* **47**, 655–684.
- Houtz RL, Nable RO, Cheniae GM.** 1988. Evidence for effects on the *in vivo* activity of ribulose-bisphosphate carboxylase/oxygenase during development of Mn toxicity in tobacco. *Plant Physiology* **86**, 1143–1149.
- Ivanov AG, Hendrickson L, Krol M, Selstam E, Öquist G, Hurry V, Hüner NPA.** 2006a. Digalactosyl-diacylglycerol deficiency impairs the capacity for photosynthetic intersystem electron transport and state transitions in *Arabidopsis thaliana* due to photosystem I acceptor-side limitations. *Plant and Cell Physiology* **47**, 1146–1157.
- Ivanov AG, Morgan R, Gray GR, Velitchkova MY, Hüner NPA.** 1998. Temperature/light dependent development of selective resistance to photoinhibition of photosystem I. *FEBS Letters* **430**, 288–292.
- Ivanov AG, Sane P, Hurry V, Krol M, Sveshnikov D, Hüner NPA, Öquist G.** 2003. Low-temperature modulation of the redox properties of the acceptor side of photosystem II: photoprotection through reaction centre quenching of excess energy. *Physiologia Plantarum* **119**, 376–383.
- Ivanov AG, Sane PV, Krol M, Gray GR, Balseris A, Savitch LV, Öquist G, Hüner NPA.** 2006b. Acclimation to temperature and irradiance modulates PSII charge recombination. *FEBS Letters* **580**, 2797–2802.
- Ivanov AG, Sane PV, Zeinalov Y, Malmberg G, Gardeström P, Hüner NPA, Öquist G.** 2001. Photosynthetic electron transport adjustments in overwintering Scots pine (*Pinus sylvestris* L.). *Planta* **213**, 575–585.
- Ivanov AG, Sane PV, Zeinalov Y, Simidjiev I, Hüner NPA, Öquist G.** 2002. Seasonal responses of photosynthetic electron transport in Scots pine (*Pinus sylvestris* L.) studied by thermoluminescence. *Planta* **215**, 457–465.
- Jordan DB, Ogren WL.** 1983. Species variation in kinetic properties of Rubisco. *Archives of Biochemistry and Biophysics* **227**, 425–433.

- Kern J, Renger G.** 2007. Photosystem II: Structure and mechanism of the water:plastoquinone oxidoreductase. *Photosynthesis Research* **94**, 183–202.
- Khabaz-Saberi H, Rengel Z, Wilson R, Setter TL.** 2010. Variation of tolerance to manganese toxicity in Australian hexaploid wheat. *Journal of Plant Nutrition and Soil Science* **173**, 103–112.
- Kitao M, Lei TT, Koike T.** 1997a. Comparison of photosynthetic responses to manganese toxicity of deciduous broad leaved trees in northern Japan. *Environmental Pollution* **97**, 113–118.
- Kitao M, Lei TT, Koike T.** 1997b. Effects of manganese toxicity on photosynthesis of white birch (*Betula platyphylla* var. *japonica*) seedlings. *Physiologia Plantarum* **101**, 249–256.
- Klughammer C, Schreiber U.** 1991. Analysis of light-induced absorbancy changes in the near-infrared spectral region. 1. Characterization of various components in isolated chloroplasts. *Zeitschrift für Naturforschung C* **46**, 233–244.
- Kohno Y, Foy CD, Fleming AL, Krizek DT.** 1984. Effect of Mn concentration on the growth and distribution of Mn and Fe in two bush bean cultivars grown in solution culture. *Journal of Plant Nutrition* **7**, 547–566.
- Kramer DM, Johnson G, Kिरात O, Edwards GE.** 2004. New fluorescence parameters for the determination of QA redox state and excitation energy fluxes. *Photosynthesis Research* **79**, 209–218.
- Krol M, Ivanov AG, Jansson S, Kloppstech K, Hüner NPA.** 1999. Greening under high light and cold temperature affects the level of xanthophyll-cycle pigments, early light-inducible proteins, and light harvesting polypeptides in wild-type barley and the Chlorina *f2* mutant. *Plant Physiology* **120**, 193–203.
- Laemmli U.** 1970. Cleavage of structural proteins during the assembly of the head of bacteriophage T4. *Nature* **227**, 680–685.
- Lei Y, Korpelainen H, Li C.** 2007. Physiological and biochemical responses to high Mn concentrations in two contrasting *Populus cathayana* populations. *Chemosphere* **68**, 686–694.
- Li Q, Chen L-S, Jiang H-X, Tang N, Yang L-T, Lin Z-H, Li Y, Yang G-H.** 2010. Effects of manganese-excess on CO₂ assimilation ribulose-1,5-bisphosphate carboxylase/oxygenase, carbohydrates and photosynthetic electron transport of leaves, and antioxidant systems of leaves and roots in *Citrus grandis* seedlings. *BMC Plant Biology* **10**, 42.
- Lidon FC, Barreiro MG, Ramalho JC.** 2004. Manganese accumulation in rice: implications for photosynthetic functioning. *Journal of Plant Physiology* **161**, 1235–1244.
- Macfie S, Taylor G.** 1992. The effects of excess manganese on photosynthetic rate and concentration of chlorophyll in *Triticum aestivum* grown in solution culture. *Physiologia Plantarum* **85**, 467–475.
- McDaniel KL, Toman FR.** 1994. Short-term effects of manganese toxicity on ribulose-1,5-bisphosphate carboxylase in tobacco chloroplasts. *Journal of Plant Nutrition* **17**, 523–536.
- Marschner H.** 1995. *Mineral nutrition of higher plants*. San Diego: Academic Press.
- Maxwell PC, Biggins J.** 1976. Role of cyclic electron transport in photosynthesis as measured by turnover of P700 *in vivo*. *Biochemistry* **15**, 3975–3981.
- Millaleo R, Reyes-Díaz M, Ivanov AG, Mora ML, Alberdi M.** 2010. Manganese as essential and toxic element for plants: Transport, accumulation and resistance mechanisms. *Journal of Soil Science and Plant Nutrition* **10**, 476–494.
- Minagawa J, Narusaka Y, Inoue Y, Satoh K.** 1999. Electron transfer between Q_A and Q_B in photosystem II is thermodynamically perturbed in phototolerant mutants of *Synechocystis* sp. PCC 6803. *Biochemistry* **38**, 770–775.
- Mora M, Rosas A, Ribera A, Rengel R.** 2009. Differential tolerance to Mn toxicity in perennial ryegrass genotypes: involvement of antioxidative enzymes and root exudation of carboxylates. *Plant and Soil* **320**, 79–89.
- Mukhopadhyay MJ, Sharma A.** 1991. Manganese in cell metabolism of higher plants. *Botanical Review* **57**, 117–149.
- Munekage Y, Hojo M, Meurer J, Endo T, Tasaka M, Shikanai T.** 2002. *PGR5* is involved in cyclic electron flow around photosystem I and is essential for photoprotection in *Arabidopsis*. *Cell* **110**, 361–371.
- Murata N, Takahashi S, Nishiyama Y, Allakhverdiev SI.** 2007. Photoinhibition of photosystem II under environmental stress. *Biochimica et Biophysica Acta* **1767**, 414–421.
- Nable RO, Houtz RL, Cheniae GM.** 1988. Early inhibition of photosynthesis during development of Mn toxicity in tobacco. *Plant Physiology* **86**, 1136–1142.
- Niyogi KK.** 1999. Photoprotection revisited: Genetic and molecular approaches. *Annual Review of Plant Physiology and Plant Molecular Biology* **50**, 333–359.
- Ohki K.** 1984. Manganese deficiency and toxicity effects on growth, development and nutrient composition in wheat. *Agronomy Journal* **76**, 213–218.
- Panda S, Mishra AK, Biswal UC.** 1987. Manganese induced peroxidation of thylakoid lipids and changes in chlorophyll- α fluorescence during aging of cell free chloroplasts in light. *Phytochemistry* **26**, 3217–3219.
- Papadakis IE, Giannakoula A, Therios IN, Bosabalidis AM, Moustakas M, Nastou A.** 2007. Mn-induced changes in leaf structure and chloroplast ultrastructure of *Citrus volkameriana* (L) plants. *Journal of Plant Physiology* **164**, 100–103.
- Powles SB.** 1984. Photoinhibition of photosynthesis induced by visible light. *Annual Review of Plant Physiology* **35**, 15–44.
- Ravenel J, Peltier G, Havaux M.** 1994. The cyclic electron pathways around photosystem I in *Chlamydomonas reinhardtii* as determined *in vivo* by photoacoustic measurements of energy storage. *Planta* **193**, 251–259.
- Rosas A, Rengel Z, Mora M.** 2007. Manganese supply and pH influence growth, carboxylate exudation and peroxidase activity of ryegrass and white clover. *Journal of Plant Nutrition* **30**, 253–270.
- Rosso D, Bode R, Li W, Krol M, Saccon D, Wang S, Schillaci LA, Rodermeil SR, Maxwell DP, Hüner NPA.** 2009. Photosynthetic redox imbalance governs leaf sectoring in the *Arabidopsis thaliana* variegation mutants *immutans*, *spotty*, *var1*, and *var2*. *The Plant Cell* **21**, 3473–3492.
- Rutherford AW, Boussac A.** 2004. Water photolysis in biology. *Science* **303**, 1782–1784.

- Sadzewka A, Carrasco M, Grez R, Mora M.** 2004. *Métodos de análisis de tejidos vegetales. Comisión de normalización y acreditación.* Sociedad Chilena de la Ciencia del Suelo (SCCS). Available at: http://www.inia.cl/platina/descarga/docs/libros/asadzewka_tejveg_2004.pdf.
- Sane PV.** 2004. Thermoluminescence: a technique for probing photosystem II. In: R Carpentier, ed, *Photosynthesis research protocols*. Totowa, NJ: Humana Press. pp 229–248.
- Sane PV, Ivanov AG, Öquist G, Hüner NPA.** 2012. Thermoluminescence. In: JJ Eaton-Rye, BC Tripathy, TD Sharkey, eds, *Photosynthesis: plastid biology, energy conversion and carbon assimilation. Advances in photosynthesis and respiration*, vol 34. Dordrecht, The Netherlands: Springer Science+Business Media. pp 445–474.
- Schaaf G, Catoni E, Fitz M, Schwake R, Schneider A, von Wirén N, Frommer WB.** 2002. A putative role for vacuolar calcium/manganese proton antiporter *AtCAX2* in heavy metal detoxification. *Plant Biology* **2**, 612–618.
- Scheller H, Haldrup A.** 2005. Photoinhibition of photosystem I. *Planta* **221**, 5–8.
- Schreiber U, Bilger W, Neubauer C.** 1994. Chlorophyll fluorescence as a noninvasive indicator for rapid assessment of in vivo photosynthesis. In: ED Schulze, MM Caldwell, eds, *Ecophysiology of photosynthesis*. Berlin: Springer-Verlag. pp 49–70.
- Sinha S, Mukherji S, Dutta J.** 2002. Effect of manganese toxicity on pigment content, Hill activity and photosynthetic rate of *Vigna radiata* L. Wilczek seedlings. *Journal of Environmental Biology* **23**, 253–257.
- Sonoike K.** 1996. Photoinhibition of photosystem I: its physiological significance in the chilling sensitivity of plants, *Plant and Cell Physiology* **37**, 239–247.
- Stoyanova Z, Poschenrieder C, Tzvetkova N, Doncheva S.** 2009. Characterization of the tolerance to excess manganese in four maize varieties. *Soil Science and Plant Nutrition* **55**, 747–753.
- Subrahmanyam D, Rathore VS.** 2000. Influence of manganese toxicity on photosynthesis in ricebean (*Vigna umbellata*) seedlings. *Photosynthetica* **38**, 449–453.
- Takahashi S, Murata N.** 2008. How do environmental stresses accelerate photoinhibition? *Trends in Plant Science* **13**, 178–182.
- Takahashi S, Milward SE, Fan DY, Chow WS, Badger MR.** 2009. How does cyclic electron flow alleviate photoinhibition in *Arabidopsis*? *Plant Physiology* **149**, 1560–1567.
- Terry N, Abadia J.** 1986. Function of iron in chloroplasts. *Journal of Plant Nutrition* **9**, 609–646.
- Towbin H, Staehelin T, Gordon J.** 1979. Electrophoretic transfer of proteins from polyacrylamide gels to nitrocellulose sheets: procedure and some applications. *Proceedings of the National Academy of Sciences, USA* **76**, 4350–4354.
- van Kooten O, Snel JFH.** 1990. The use of chlorophyll fluorescence nomenclature in plant stress physiology. *Photosynthesis Research* **25**, 147–150.
- Vass I, Govindjee.** 1996. Thermoluminescence from the photosynthetic apparatus. *Photosynthesis Research* **48**, 117–126.
- Vaughn KC, Duke SO.** 1984. Function of polyphenol oxidase in higher plants. *Physiologia Plantarum* **60**, 106–112.